Schwarz and Dirichlet–Neumann Waveform Relaxation for a Stefan Problem

Ronald D. Haynes[0000−0002−4804−3152],
Martin J. Gander[0000−0001−8450−9223]

1 Introduction

There have been a lot of research efforts over the past two decades to solve space-time problems in parallel on large scale HPC architectures. New algorithms for the parallelization in time (PinT) have been developed, see the recent research monograph [10] and references therein, and are tested on large scale problems, see e.g. [17], and also the historical introduction [6]. The authors are currently developing PinT methods to solve free-boundary problems. In particular, we are interested here in PinT algorithms for Stefan problems, for which we will introduce and study numerically two algorithms, namely Schwarz Waveform Relaxation (SWR), introduced in DD9 [5] and named in [12], and Dirichlet-Neumann Waveform Relaxation (DNWR) introduced in [8].

The classical one-phase Stefan problem in one spatial dimension, see Figure 1 for the geometry, involves finding the temperature $u(x,t)$ and the interface $s(t)$ satisfying

$$\begin{aligned} u_t &= u_{xx} \quad \text{in } \Omega := (0, s(t)) \times (0, T], & s_t &= -u_x(s(t), t), \\ u(x, 0) &= 0, & s(0) &= b > 0, \\ u_x(0, t) &= -h(t), \ h(t) \geq 0, \ u(s(t), t) = 0. \end{aligned} \tag{1}$$

For example the function $u(x,t)$ may represent the temperature of water, and $s(t)$ is the moving boundary (or free boundary) that separates the liquid and the melting ice. The Neumann condition at $x = 0$ models a heat flux into the domain. Physically, $u_x(0,t) < 0$ means that the temperature of the water will increase, resulting in ice melt. So we expect $s(t)$ to be monotonically increasing.

Ronald D. Haynes
Memorial University of Newfoundland, Canada, e-mail: rhaynes@mun.ca

Martin J. Gander
University of Geneva, Switzerland, e-mail: martin.gander@unige.ch

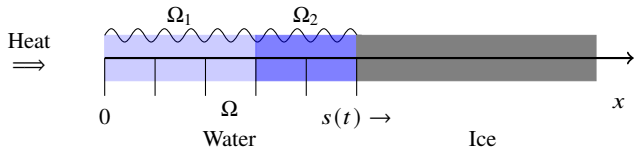

Fig. 1 Geometry of the melting problem with heat from the left melting ice ($x > s(t)$) and turning it into water ($\Omega = \Omega_1 \cup \Omega_2$ with Ω_1 and Ω_2 defined precisely in Section 3), moving the interface position $s(t)$ over time to the right.

Defining the set $Q(s,T) = \{(x,t)|0 < x < s(t), 0 < t < T\}$, we seek a (strong) solution satisfying (1) with $s \in C^1([0,T])$, $u \in C(\overline{Q_{s,T}}) \cap C^{2,1}(Q_{s,T})$, $u_x \in C(\overline{Q_{s,T}} - \{t = 0\})$. We assume the flux, $h(t)$, satisfies $h \in C([0,T])$, $h(t) > 0$, $0 \le t \le T$, and the initial condition satisfies $u_0(x) \in C([0,b]), 0 \le u_0(x) \le H(b-x)$, $0 \le x \le b$, for some constant $H > 0$.

2 Background

There has been a long history of research on the one-phase Stefan problem, starting with the work of Stefan [18]. Stefan was actually interested in the (reverse) problem of ice growth. The problem has been studied in various contexts, including existence and uniqueness of solutions (see Evans [4] and later extensions by Douglas and Kyer [3, 16], as well as stability of the interface [1], and the analysis of numerical approaches.

Numerically, it is convenient to solve the problem on a fixed domain $\Omega_\xi := (0,1)$ by introducing the change of variables $\xi = x/s(t)$ for $t > 0$. The chain rule then gives the fixed domain formulation for $\hat{u}(\xi,t) := u(x(\xi),t)$ as

$$\begin{aligned} \hat{u}_t &= \tfrac{\xi}{s} s_t \hat{u}_\xi + \tfrac{1}{s^2}\hat{u}_{\xi\xi} \qquad \text{in } \Omega_\xi \times \{t > 0\}, \qquad & s_t &= -\tfrac{1}{s}\hat{u}_\xi(1,t), \\ \hat{u}(\xi,0) &= 0, & s(0) &= b > 0, \\ \hat{u}_x(0,t) &= -s(t)h(t),\ \hat{u}(1,t) = 0. \end{aligned} \tag{2}$$

There are two main options to compute the single domain or global solution – determine $\hat{u}$ and s simultaneously (by solving the coupled system (2)) or we can explicitly decouple the system, first solving the $\hat{u}$ equation with a fixed initial guess for the s and then updating the interface using the s equation, updating $\hat{u}$, and so on. This latter approach was used by Evans [4] in his existence proof.

3 Schwarz and Dirichlet-Neumann waveform relaxation

The iterations we consider impose the transmission conditions at the interface(s) in the fixed computational co-ordinate ξ, $0 < \xi < 1$. We split the computational space-time domain, $\hat{\Omega} := (0,1) \times (0,T]$, into two (possibly) non-overlapping subdomains $\hat{\Omega}_1 := (0, \hat{\beta}) \times (0,T]$ and $\hat{\Omega}_2 := (\hat{\alpha}, 1) \times (0,T]$ where $0 < \hat{\alpha} \leq \hat{\beta} < 1$. We assume that $\hat{\alpha}$ and $\hat{\beta}$ are fixed. We denote the DD solutions on $\hat{\Omega}_1$ and $\hat{\Omega}_2$ as $\hat{u}_1^k$ and $\hat{u}_2^k$, respectively.

The Schwarz waveform relaxation (SWR) algorithm [5, 12] computes sequences of subdomain solutions $\{\hat{u}_1^k, \hat{u}_2^k\}$, approximate interfaces $\{s^k\}$ and grid transformations $\{x^k\}$ which we hope converge to $\hat{u}_1$ and $\hat{u}_2$ (the restrictions of the global solution $\hat{u}$ to $\hat{\Omega}_1$ and $\hat{\Omega}_2$), to s (the location of the true interface) and to x (the grid transformation satisfying $x = \xi s$). In the SWR setting we can choose to compute the interface implicitly with the right-most subdomain solve, or update it after the subdomain solutions have been computed.

This splitting approach in the fixed computational co-ordinate ξ is motivated, in part, by a similar domain decomposition approach first proposed in [13] and then studied theoretically in [7, 14, 15] for the generation of an unknown mesh transformation $x(\xi)$ using r-refinement.

Suppose an initial guess for the interface, $s^1(t)$, with $s^1(0) = b > 0$, and an initial guess for $\hat{u}_2^0(\hat{\beta}, t)$ for $t \geq 0$ are given. If the solves on each subdomain are handled **explicitly** then the alternating classical SWR iteration in **computational co-ordinates** proceeds as, for $k = 1, 2, \ldots$ solve for $\hat{u}_1^k$ in $\hat{\Omega}_1$ and $\hat{u}_2^k$ in $\hat{\Omega}_2$ satisfying

$$\begin{aligned}
\partial_t \hat{u}_1^k &= \tfrac{\xi}{s^k} \partial_t s^k \partial_\xi \hat{u}_1^k + \tfrac{1}{(s^k)^2} \partial_{\xi\xi} \hat{u}_1^k, & \partial_t \hat{u}_2^k &= \tfrac{\xi}{s^k} \partial_t s^k \partial_\xi \hat{u}_2^k + \tfrac{1}{(s^k)^2} \partial_{\xi\xi} \hat{u}_2^k, \\
\hat{u}_1^k(\xi, 0) &= 0, & \hat{u}_2^k(\xi, 0) &= 0, \\
\hat{u}_{1\xi}^k(0, t) &= -s^k(t) h(t), & \hat{u}_2^k(1, t) &= 0, \\
\hat{u}_1^k(\hat{\beta}, t) &= \hat{u}_2^{k-1}(\hat{\beta}, t), & \hat{u}_2^k(\hat{\alpha}, t) &= \hat{u}_1^k(\hat{\alpha}, t).
\end{aligned} \tag{3}$$

In this iteration the subdomains are overlapping, ie. $\hat{\alpha} < \hat{\beta}$, and this is followed by explicitly updating the interface position from s^k to s^{k+1} by solving

$$\frac{ds^{k+1}}{dt} = -\frac{1}{s^k} \partial_\xi \hat{u}_2^k(1, t), \quad s^{k+1}(0) = b. \tag{4}$$

The kth approximate grid transformations, x^k, (obtained at the kth Schwarz iteration) satisfies

$$x_j^k = \xi_j s^k(t), \qquad \text{for} \quad j = 0, 1, \ldots, N, \quad \text{and} \quad k = 0, 1, 2, \ldots.$$

In **physical co-ordinates** this iteration is equivalent to solving the subdomain problems for u_1^k in $(0, \hat{\alpha} s^k(t)) \times (0,T]$ and u_2^k in $(\hat{\alpha} s^k(t), s^k(t)) \times (0,T]$ satisfying

$$\begin{aligned}
\partial_t u_1^k &= \partial_{xx} u_1^k & \partial_t u_2^k &= \partial_{xx} u_2^k \\
u_1^k(x,0) &= 0, & u_2^k(x,0) &= 0, \\
\partial_x u_{1x}^k(0,t) &= -h(t), & u_2^k(\hat{\alpha} s^k, t) &= u_1^k(\hat{\alpha} s^k, t), \\
u_1^k(\hat{\beta} s^k(t), t) &= u_2^{k-1}(\hat{\beta} s^{k-1}(t), t), & u_2^k(s^k(t), t) &= 0,
\end{aligned}$$

followed by updating the interface position as in (4).

An alternative is to handle the subdomain solves on $\hat{\Omega}_2$ **implicitly**, which would simultaneously update $\hat{u}_2^k$ and s^{k+1}. In this case the problem solved on $\hat{\Omega}_1$ is identical to that in (3). The subdomain problem on $\hat{\Omega}_2$ becomes

$$\begin{aligned}
\partial_t \hat{u}_2^k &= \frac{\xi}{s^{k+1}} \partial_t s^{k+1} \partial_\xi \hat{u}_2^k + \frac{1}{(s^{k+1})^2} \partial_{\xi\xi} \hat{u}_2^k, & s_t^{k+1} &= -\frac{1}{s^{k+1}} \hat{u}_{2\xi}^k(1,t), \\
h u_2^k(\xi, 0) &= 0, & s^{k+1}(0) &= b, \\
\hat{u}_2^k(1,t) &= 0, \hat{u}_2^k(\hat{\alpha}, t) = \hat{u}_1^k(\hat{\alpha}, t),
\end{aligned}$$

With the parameter values chosen in our tests, we have found that this implicit treatment of the right-most subdomain only improves convergence for the first few iterations (depending on initial guesses for the solution and interface), so we will not consider it further here.

To avoid the overlap in the subdomains (ie. choosing $\hat{\alpha} = \hat{\beta}$) we consider a Dirichlet-Neumann SWR method [8]. In **computational co-ordinates** this alternating iteration proceeds as, for $k = 0, 1, 2, \ldots$ solve for $\hat{u}_1^k$ on $\hat{\Omega}_1$ and $\hat{u}_2^k$ on $\hat{\Omega}_2$ satisfying

$$\begin{aligned}
\partial_t \hat{u}_1^k &= \tfrac{\xi}{s^k} \partial_t s^k \partial_\xi \hat{u}_1^k + \tfrac{1}{(s^k)^2} \partial_{\xi\xi} \hat{u}_1^k & \partial_t \hat{u}_2^k &= \tfrac{\xi}{s^k} \partial_t s^k \partial_\xi \hat{u}_2^k + \tfrac{1}{(s^k)^2} \partial_{\xi\xi} \hat{u}_2^k, \\
\hat{u}_1^k(\xi, 0) &= 0, & \hat{u}_2^k(\xi, 0) &= 0, \\
\hat{u}_{1\xi}^k(0,t) &= -s^k(t) h(t), & \hat{u}_{2\xi}^k(\hat{\alpha}, t) &= \hat{u}_{1\xi}^k(\hat{\alpha}, t), \\
\hat{u}_1^k(\hat{\alpha}, t) &= \hat{h}^k(t), & \hat{u}_2^k(1,t) &= 0,
\end{aligned} \tag{5}$$

where $\hat{h}^k(t) = \theta \hat{u}_2^{k-1}(\hat{\alpha}, t) + (1-\theta)\hat{h}^{k-1}(t)$. This is followed by explicitly updating the interface position from s^k to s^{k+1} by solving

$$\frac{ds^{k+1}}{dt} = -\frac{1}{s^k} \partial_\xi \hat{u}_2^k(1,t), \quad s^{k+1}(0) = b. \tag{6}$$

In **physical co-ordinates** this iteration is equivalent to solving the subdomain problems for u_1^k and u_2^k satisfying

$$\begin{aligned}
\partial_t u_1^k &= \partial_{xx} u_1^k & \partial_t u_2^k &= \partial_{xx} u_2^k \\
u_1^k(x,0) &= 0, & u_2^k(x,0) &= 0, \\
\partial_x u_1^k(0,t) &= -h(t) & u_{2x}^k(\hat{\alpha} s^k(t), t) &= u_{1x}^k(\hat{\alpha} s^k(t), t) \\
u_1^k(\hat{\alpha} s^k(t), t) &= h^k(t), & u_2^k(s^{k+1}(t), t) &= 0,
\end{aligned}$$

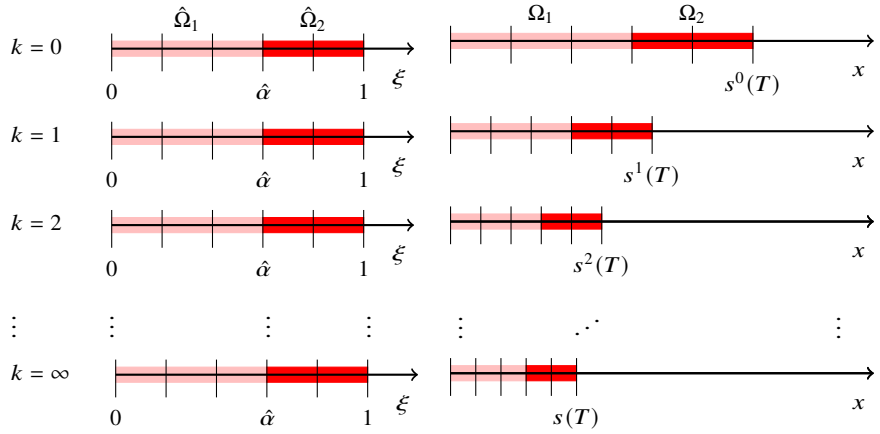

Fig. 2 Non-overlapping subdomain partitioning in the two co-ordinate systems, ξ–coordinates (left) and x–coordinates (right), at a fixed time, $T > 0$, as the Schwarz iteration counter, k, is increasing.

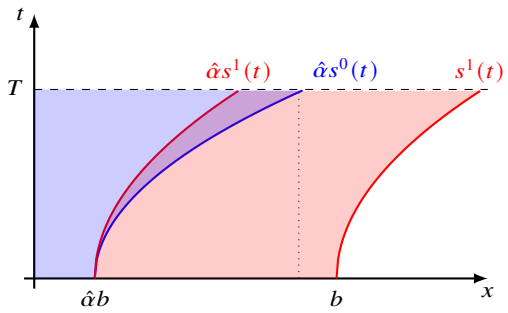

Fig. 3 Two non-overlapping domains at different Schwarz iterates, viewed in physical coordinates.

where $h^k(t) = \theta u_2^{k-1}(\hat{\alpha}s^{k-1}(t), t) + (1-\theta)h^{k-1}(t)$.

Figure 2 provides a cartoon of the non-overlapping subdomains as viewed in the computational and physical co-ordinates. The subdomains in the computational co-ordinates are fixed in size and location for all Schwarz iterations as shown in the left of Figure 2. Figure 2 (right) shows this is not the case in physical co-ordinates. At the discrete level, our implementation does keep the **number** of mesh points fixed in the physical domains. In Figure 2 (right) we also see the sequence $s^0(T), s^1(T), \ldots$ converging to $s(T)$ where $T > 0$ is the final computational time.

The space-time subdomains in physical co-ordinates are shown in Figure 3. If one compares the partitioning of the space-time domain between Schwarz iterates, $s^k(t)$ and $s^{k+1}(t)$, these will not match and will manifest as overlaps in physical space.

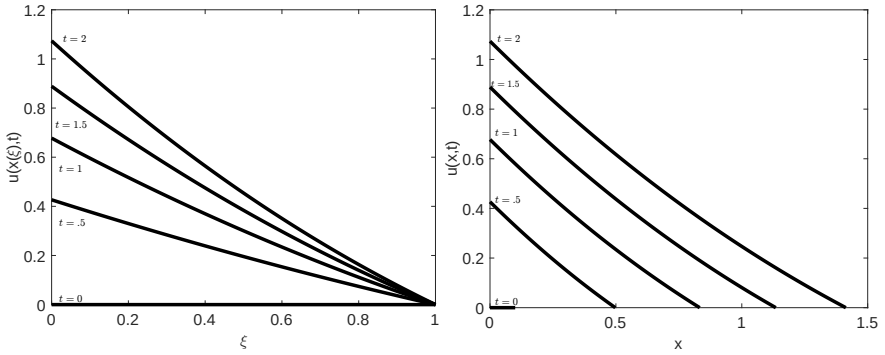

Fig. 4 Solutions to the Neumann Stefan Problem in computational (left) and physical (right) co-ordinates.

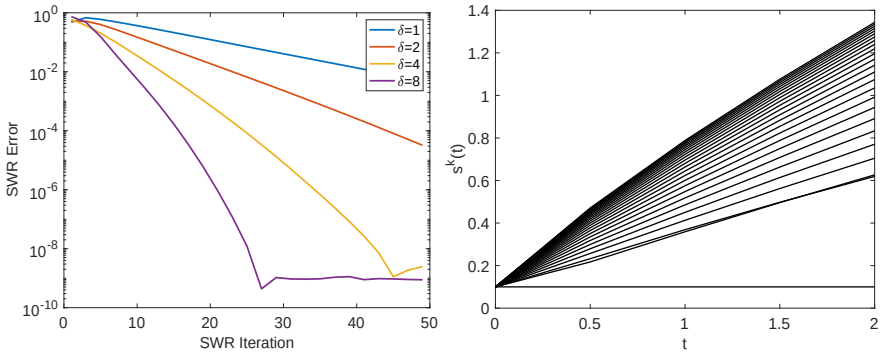

Fig. 5 Left: Convergence histories for classical SWR applied to a Neumann Stefan problem for various overlaps, δ. Right: Interface approximations obtained during each classical SWR iteration.

4 Numerical Results

To illustrate the performance of the two waveform relaxation algorithms, we consider a Stefan problem with $h(t) = 1$ and $b = 0.1$. In Figure 4 we show the global solutions obtained by solving the model problem (2) discretized using centered finite differences in ξ and backward Euler in time. On the left we show spatial snapshots of the solution in computational co-ordinates at various times and on the right we show the solution in physical co-ordinates. The movement of the interface is clearly visible in the physical co-ordinates as the domain of each snapshot increases with time.

In Figure 5 (left) we show convergence histories for the classical SWR algorithm for various overlaps, $\delta = \hat{\beta} - \hat{\alpha}$. The convergence is measured in terms of the maximum difference between successive interface approximations, ie. $\max_{0\le t\le T} |s^{k+1}(t) - s^k(t)|$. We see that the convergence is very slow for small overlaps and improves as the overlap increases. In Figure 5 (right) we show the interface approximations obtained during each classical SWR iteration for an overlap of

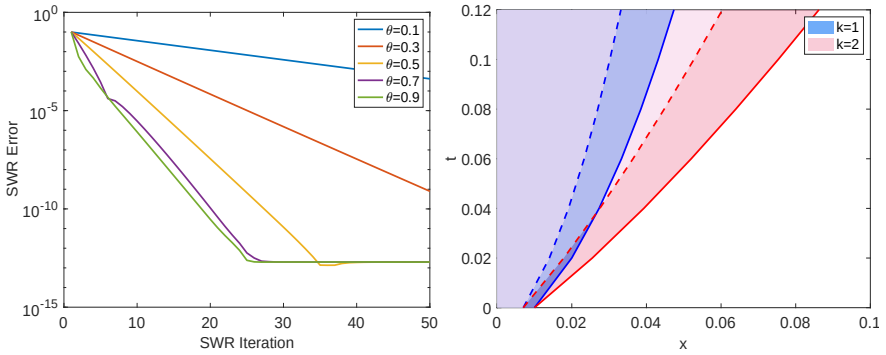

Fig. 6 Left: Convergence histories for DNWR applied to a Neumann Stefan problem for various overlaps. Right: The non-overlapping domains in physical co-ordinates during the first two DNWR iterations.

$\delta = 1$. The iteration is started with $s^0(t) = b$. We see that the approximate interfaces converge to the true interface, shown in black.

Finally, in Figure 6 (left) we show convergence histories for the DNWR algorithm for various values of the relaxation parameter, θ. We see that with no overlap fast convergence is recovered with appropriate choices of θ. In Figure 6 (right) we show the subdomains in physical co-ordinates for the first two DNWR iterations. The blue-purple subdomains are Ω_1 and Ω_2 during the first iteration. The interface position is then updated giving Ω_1 and Ω_2 in pink-lightpink during the second iteration. The dashed curves are the images, in physical co-ordinates, of the fixed interface in computational co-ordinates.

5 Conclusions

We have presented two waveform relaxation algorithms to solve one phase Stefan problems. The first is a classical SWR algorithm which requires overlapping subdomains. The second is a Dirichlet-Neumann SWR algorithm which does not require overlap. Numerical results illustrate the performance of both algorithms.

There are many research directions to pursue for such space-time algorithms for the Stefan problem: a first step are the theoretical study of these iterations, which will appear elsewhere. A second step is to consider optimized SWR, which can also be run without overlap, like DNWR, and for which the optimization of the transmission conditions gives an entirely new set of min-max problems to study. One can then also consider Neumann-Neumann waveform relaxation algorithms for Stefan problems. And finally, waveform relaxation techniques are just one class of PinT algorithms, one can also consider Parareal type methods for the Stefan Problem, see already [2], or space-time multigrid (STMG), or even direct space-time parallel methods like ParaDiag [9], and the review [11].

Acknowledgements The authors would like to thank Felix Kwok for discussions about the implementation.

Competing Interests The authors have no conflicts of interest to declare that are relevant to the content of this chapter.

References

1. Cannon, J., Douglas, J.: The stability of the boundary in a Stefan problem. Annali Della Scuola Normale Superiore Di Pisa-classe Di Scienze **21**(1), 83–91 (1967)
2. Diao, P.: The Parareal Algorithm Applied to the Stefan Problem. Ph.D. thesis, Florida State University (2020)
3. Douglas, J.: A uniqueness theorem for the solution of a Stefan problem. Proc. Am. Math. Soc. **8**(2), 402 (1957)
4. Evans II, G.: A note on the existence of a solution to a problem of Stefan. Quart. Appl. Math. **9**(2), 185–193 (1951)
5. Gander, M.J.: Overlapping Schwarz for linear and nonlinear parabolic problems. In: Proceedings of the 9th International Conference on Domain decomposition, pp. 97–104 (1996)
6. Gander, M.J.: 50 years of time parallel time integration. In: Multiple Shooting and Time Domain Decomposition Methods: MuS-TDD, Heidelberg, May 6-8, 2013, pp. 69–113. Springer (2015)
7. Gander, M.J., Haynes, R.D.: Domain decomposition approaches for mesh generation via the equidistribution principle. SIAM J. Numer. Anal. **50**(4), 2111–2135 (2012)
8. Gander, M.J., Kwok, F., Mandal, B.C.: Dirichlet-Neumann and Neumann-Neumann waveform relaxation algorithms for parabolic problems. ETNA **45**, 424–456 (2016)
9. Gander, M.J., Liu, J., Wu, S.L., Yue, X., Zhou, T.: Paradiag: Parallel-in-time algorithms based on the diagonalization technique. arXiv preprint arXiv:2005.09158 (2020)
10. Gander, M.J., Lunet, T.: Time Parallel Time Integration. SIAM (2024)
11. Gander, M.J., Wu, S.L., Zhou, T.: Time parallelization for hyperbolic and parabolic problems. Acta Numer. **34**, 385–489 (2025)
12. Gander, M.J., Zhao, H.: Overlapping Schwarz waveform relaxation for parabolic problems in higher dimension. In: Proceedings of Algoritmy, vol. 14, pp. 42–51 (1997)
13. Haynes, R.D.: Recent Advances in Schwarz Waveform Moving Mesh Methods – A New Moving Subdomain Method. In: Y. Huang, R. Kornhuber, O. Widlund, J. Xu (eds.) Domain Decomposition Methods in Science and Engineering XIX, pp. 253–260. Springer Berlin Heidelberg, Berlin, Heidelberg (2011)
14. Haynes, R.D., Howse, A.J.M.: Alternating Schwarz methods for partial differential equation-based mesh generation. Int. J. Comput. Math. **92**(2), 349–376 (2015)
15. Haynes, R.D., Kwok, F.: Discrete analysis of domain decomposition approaches for mesh generation via the equidistribution principle. Math. Comput. **86**(303), 233–273 (2016)
16. Kyner, W.: An existence and uniqueness theorem for a nonlinear Stefan problem. Indiana Univ. Math. J. **8**(4), 483–498 (1959)
17. Ong, B.W., Schroder, J.B.: Applications of time parallelization. Comput. Vis. Sci. **23**(1), 11 (2020)
18. Stefan, J.: Über einige Probleme der Theorie der Wärmeleitung. Sitzungber., Wien, Akad. Mat. Natur **98**, 473–484 (1889)